Materials and Design 59 (2014) 151–159

Contents lists available at ScienceDirect

Materials and Design

journal homepage: www.elsevier.com/locate/matdes

Technical Report

Studies on the formability of powder metallurgical aluminum–copper composite

Desalegn Wogaso Wolla [a,*], M.J. Davidson [a], A.K. Khanra [b]

[a] Department of Mechanical Engineering, National Institute of Technology, Warangal 506 004, Andhra Pradesh, India
[b] Department of Metallurgical and Materials Engineering, National Institute of Technology, Warangal 506 004, Andhra Pradesh, India

ARTICLE INFO

Article history:
Received 22 November 2013
Accepted 21 February 2014
Available online 3 March 2014

ABSTRACT

Formability is concerned with the extent of deformation that the materials undergo before failure; thus its investigation is critical for successful processing of materials during bulk deformation. The present investigation has been undertaken to generate the forming limit diagrams for powder metallurgical aluminium–copper composites for different initial relative densities and copper contents. Sintered aluminium–copper composite compacts of 2%, 4% and 6% copper content with different initial relative densities have been prepared by applying recommended powder compaction pressures. The material properties such as apparent strain hardening exponent and strength coefficient were determined using stage wise compression test to generate the formability limit diagram. Densification curves were plotted to investigate the effect of initial relative density and copper content on the pore closure phenomena during deformation. Theoretical and experimental investigations using standard ring compression test were carried out to determine friction factor between tool and work piece interfaces for different initial relative density and copper content. The critical transition densities vide the forming limit diagram were found to be 84%, 85.3%, 86% and 87.5% for pure sintered aluminium, Al–2%Cu, Al–4%Cu and Al–6%Cu composites respectively. The friction factor between tool and work piece interfaces has showed increasing pattern for all the cases with decrease in the initial relative density and increase in the copper content of the composite.

1. Introduction

Powder metallurgical (PM) components have superior properties than parts made through other manufacturing processes. It is rapid, economical and high volume production method for making parts from powders. This route yields products with higher strength, wear resistance and close dimensional tolerance. It involves various steps: powder mixing or blending, compaction and sintering.

Nowadays, numerous secondary processing techniques have been used to enhance the reduced mechanical properties of PM components due to the presence of residual porosity left after sintering. Precision cold forming can result in higher production of parts with good dimensional control and good surface finish [1]. It is often possible to use cheaper materials with low alloy content because of extensive strain hardening during cold forming. It is also reported [2] that cold working is one of the methods to promote strength in which the strain induced will be the prominent factor for strengthening wrought materials. The same is true for PM materials too; however the additional factor that governs the work hardening behaviour is the pore closure phenomena.

In metal forming operations, formability of a material is crucial technological concept that mainly depends on the ductility of the material and associated process parameters. Several authors [3–7] investigated workability and/or effects of process parameters on the workability of PM aluminum and/or aluminum metal composites. Narayansamy et al. [5] studied the workability of Al–Al_2O_3 PM composite on cold upsetting and observed that the workability of a material purely depends on the amount of ductile fracture present in the material. Raj et al. [8] presented an experimental investigation on the effect of different percentage of carbon and manganese on the workability and strain hardening behaviour of Fe–C–Mn sintered composites during cold upsetting. They observed better workability for a composition of Fe–0.1C–0.5Mn because of higher initial fractional density and pore closure phenomena.

Forming limit diagram (FLD) is a valuable tool for analyzing the deformation mechanics of metal forming. It has been used as a reference to estimate how the material close to failure. Chakravarthy et al. [9] investigated the influence of temperature on the FLD of sintered PM performs through determining the critical transition

* Corresponding author. Tel.: +91 956 0476165; fax: +91 870 2459547.
E-mail addresses: desalegnnitw@gmail.com, desalegnwogaso@nitw.ac.in (D.W. Wolla).

http://dx.doi.org/10.1016/j.matdes.2014.02.049
0261-3069/

density (CTD) vide the diagram. The CTD separates the safe working zone from the fail zone in further processing of the materials to produce crack free products. The results of previous works [10–12] present that formability of cold extrudates are significantly dependent on the initial relative density of deformed PM materials. Since all the stresses acting during cold extrusion are compressive, the extrudates have better mechanical properties and density nearer to the corresponding wrought materials.

According to Narayanasamy et al. [13], the work hardening behavior of PM preforms comprises of both the effect of geometric hardening and matrix hardening. Thus persistent pore closure phenomena and matrix hardening are considered during the determination of strain hardening exponent and strength coefficient for PM materials. The general Ludwik equation for fully dense materials is given as $\sigma = K\varepsilon^n$, where σ is the true stress, ε is the true strain, K is the strength coefficient and n is strain hardening exponent. Correspondingly, the flow stress equation for the PM preforms can be equivalently given as $\sigma = K_a\bar{\varepsilon}^{n_a}$, where K_a is the apparent strength coefficient and n_a is the apparent strain hardening exponent. Both the apparent strength coefficient and apparent strain hardening exponent are functions of the relative density of sintered preforms [14].

According to the FLD generated by Chakravarthy et al. [9], the variations of K_a and n_a against initial relative density are used to determine the CTD of the PM preforms which determines the minimum initial relative density to obtain crack free cold extrudates. The CTD value exists at the transition point on the slope of linear plot of K_a and n_a values for different initial relative densities of the preforms. It determines the formability of sintered PM preforms during cod extrusion. Das et al. [15] conducted experimental research on the effect of the reinforcement particles on the forgeability and mechanical properties of aluminum-metal composite and observed that the forgeability of the material is greatly dependent on the weight percentage of the reinforcement particles. Further research was performed by Madhusudan et al. [16] on fabrication and deformation studies on aluminum–copper composite metallic materials and reveled that when the weight percentage of copper reinforcement increases, the composite undergoes early fracture.

Literatures related to the formability study of sintered aluminum–copper composite is limited though the material has got popularity in major industrial applications as air-craft structures, rivets, hardware, truck wheels and screw-machine products as described by Mondolfo et al. [17]. It is relevant to determine the formability of the material through generating the FLD. The present research makes an attempt to generate the FLD for sintered aluminium–copper composite of various initial relative densities and content of copper in the composite. Thus the effect of initial relative density and content of copper on the CTD which demarcates the safe and fail zone for cold forming of sintered aluminum–copper composites are explored. Since friction affects the formability, deformation load, product surface quality and dies wear characteristics, evaluation of the effect of initial relative density and the content of copper on the friction factor is other vital part of the current research. The author expects shift in the values of CTDs and change in the friction factor (m) values due to change in processing conditions throughout the investigation.

2. Experimental details

2.1. Specimen preparation

To investigate the deformation mechanisms in the present work, the porous specimens were prepared from atomized aluminum and copper powders of each −325 μm mesh size. Aluminum powder has 99% pure and a maximum of 0.53% insoluble impurity limit whereas copper powder has minimum of 99% pure and maximum limit of impurities are 0.5% and 0.03% of iron (Fe) and heavy metals (Pb) respectively. The scanning electron microscope (SEM) photographs of aluminum and copper powder are shown in Figs. 1a and 1b respectively.

The PM preforms were prepared from pure aluminum powder and aluminium–copper mix with addition of 2%, 4% and 6% (by weight) copper in the composite to obtain dimensions of 12.5 mm in height and 15 mm in diameter. A pot mill was used

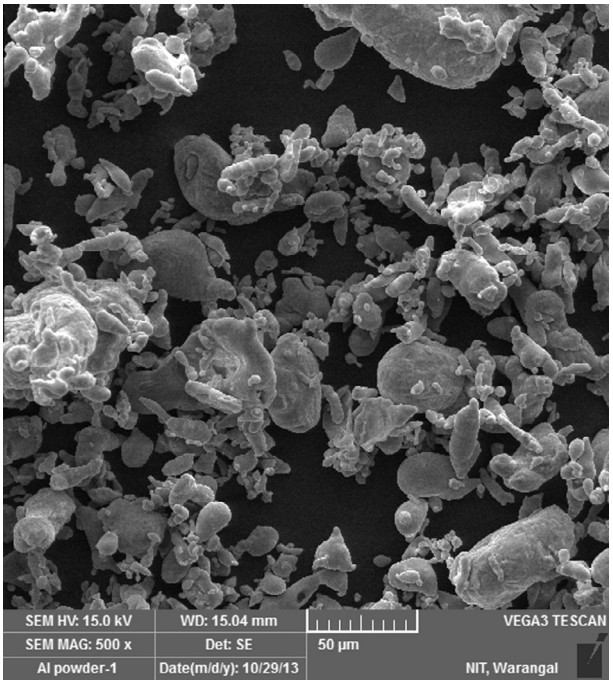

Fig. 1a. The SEM photograph of aluminium powder.

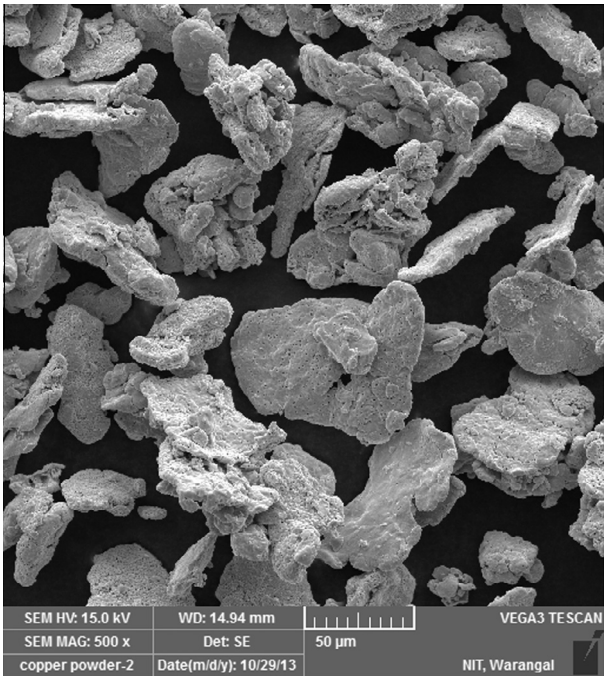

Fig. 1b. The SEM photograph of copper powder.

for blending and mixing the powder to obtain uniformly distributed aluminum and copper powder mix. Compacts of different initial relative densities were made by using recommended compaction pressure that ranges from 110 MPa–423 MPa. Zinc stearate was applied for lubricating the die, punch and butt during compaction. A uniaxial compaction was employed for compacting properly poured powder in the die. The compacts were sintered in a muffle furnace at 550 ± 10 °C for holding period of 45 min. Immediately after the completion of the sintering schedule, the specimens were allowed to cool to room temperature inside the furnace by switching off the power source of the furnace.

2.2. Deformation test

Initial dimensions of the specimens such as height (H_0), diameter (D_0) and initial relative density (ρ_0) were measured and recorded. The Archimedes principle was utilized to measure the density of the compacts. The deformation of the specimens was conducted between two flat platens on a hydraulic press of 0.5 MN capacity. Each specimen was subjected to incremental loadings until the appearance of the first visible crack on the free surface. For each test, 6–8 specimens of the same dimensions were taken and deformed to different strain levels. After the deformation, dimensional changes such as final height (H_f), top contact diameter (D_{tc}), bottom contact diameter (D_{bc}), bulged diameter (D_b) and density of the preforms were measured. The above measurements, before and after deformation, are illustrated in Fig. 2a, and the photographs of the actual deformed samples are shown in Fig. 2b.

2.3. Ring compression test

The experiment was conducted for Al and Al–Cu PM composite with different content of copper (2%, 4% and 6%) in the composite for initial relative density ranging from 81% to 93%. Standard ring compression specimen of OD: ID: H = 6:3:2 (20: 10: 6.67 mm), where OD is the outer diameter, ID is the internal diameter and H is the height of the specimen, were prepared by machining from sintered compacts. These samples were deformed under two parallel platens at ram speed of 0.5 mm/min in 4–6 stages. The specimen after each stage of deformation was cleaned for the next stage of deformation. The friction factor, m, was determined from the reduction in the internal diameter of the ring (%) and reduction in height (%) and made to fit the Male and Cockcroft [18] friction calibration curve. The finite element method (FEM) software, DEFORM 2D, was used for establishing the Male and Cockcroft calibration curve. The flow stress equation ($\sigma = K_a \varepsilon^{n_a}$) was

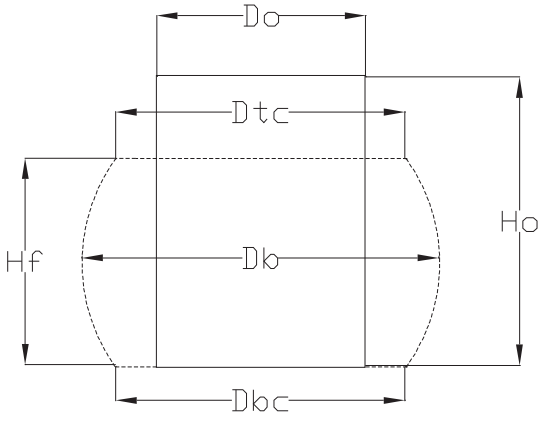

Fig. 2a. Upset forging test preform geometry before and after deformation.

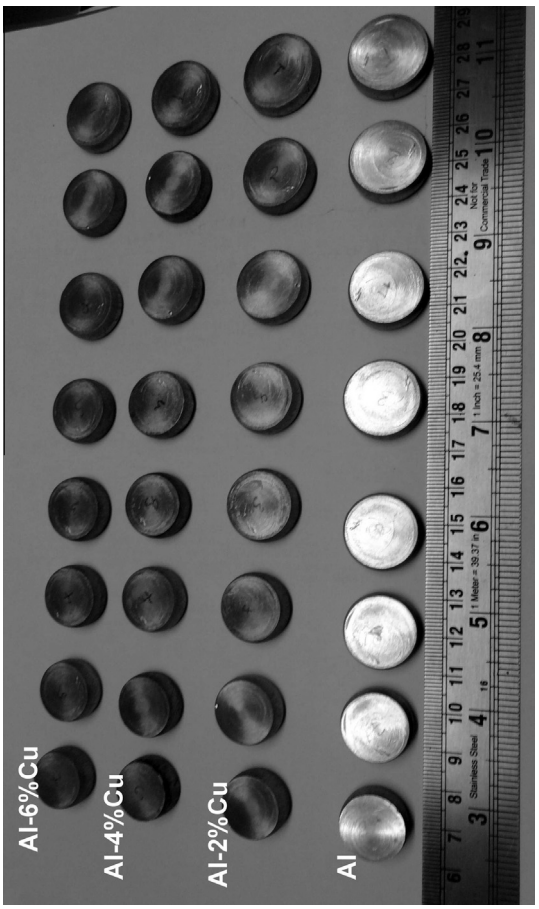

Fig. 2b. Photograph of actual deformed samples of sintered Al, Al–2%Cu, Al–4%Cu and Al–6%Cu PM made at 527 MPa compaction pressure.

ascertained using solid cylindrical disc compression test in the current work for different content of copper and initial relative densities. The K_a and n_a values obtained from this test were given as input to the FEM software (DEFORM 2D).

To determine the friction factor (m) theoretically, the values of the initial undeformed geometries and the changes in the dimensions after deformation were used in the following equations presented in references [19–21].

$$m = \frac{-1}{2\frac{R_0}{T}\left(1+\frac{R_i}{R_0}-2\frac{R_n}{R_0}\right)} \times \ln\left[\left(\frac{R_i}{R_0}\right)^2 \times \frac{\left(\frac{R_n}{R_0}\right)^2+\sqrt{3+\left(\frac{R_n}{R_0}\right)^4}}{\left(\frac{R_n}{R_0}\right)^2+\sqrt{3\left(\frac{R_i}{R_0}\right)^4+\left(\frac{R_n}{R_0}\right)^2}}\right] \quad (1)$$

$$R_n = R_0\sqrt{\frac{\left(\frac{R_i}{R_0}\right)+\left(\frac{\Delta R_i}{\Delta R_0}\right)}{\left(\frac{R_0}{R_i}\right)+\left(\frac{\Delta R_i}{\Delta R_0}\right)}} \quad (2)$$

$$\mu = \frac{m}{\sqrt{3}} \quad (3)$$

R_n is the mean radius of specimen, R_i is the inner radius of specimen after deformation, R_o is the external radius of the specimen after deformation, ΔR_i is the change in the internal radius of the specimen, ΔR_0 is the change in the external radius of the specimen, T is the height of the specimen, m is the friction factor, μ is the coefficient of friction.

3. Result and discussion

3.1. Densification

During the stage wise deformation of PM parts, such as carried out in this research, different authors observed increase in the densification [2,22] of the preforms due to induced axial strain. Figs. 3a–3d have been plotted between relative density and induced axial strain to show the densification behavior of the preforms for different initial relative densities and amount of copper content in the composite.

It is clearly evident that the relative density increased persistently with the induced axial strain. The increase in densification during deformation is the result of increased lateral flow of materials due to friction that results in increased formation of hydrostatic stress. The presence of compressive hydrostatic stress in the PM parts plays a significant role in the pore closure phenomena. It depends on the amount of porosity, material property and the friction condition between the tool and work piece interfaces. The amount of densification is different for different values of initial relative densities and amount of copper content in the composite as it is shown in the densification curves. Preforms with lesser initial relative density values showed higher values of densification rate. This is due to increased amount of hydrostatic stress generated for the closure of more number of pores that

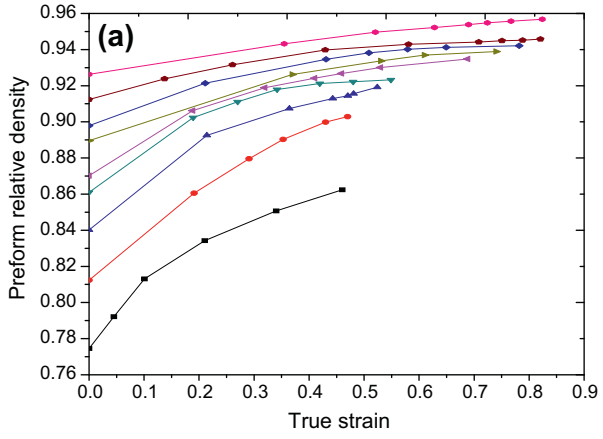

Fig. 3a. Variation of relative density with respect to true strain for PM aluminium preforms.

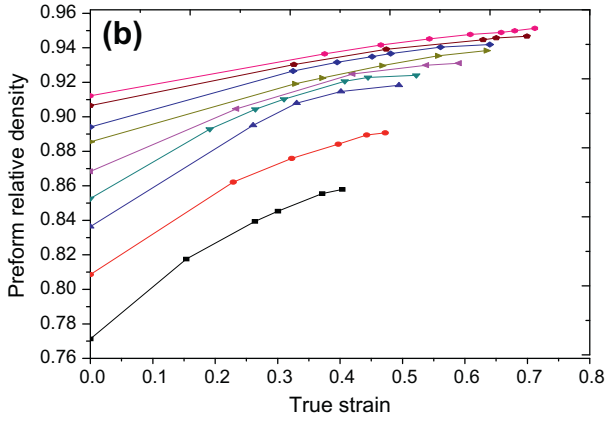

Fig. 3b. Variation of the relative density with respect to true strain for PM Al–2%Cu composite preforms.

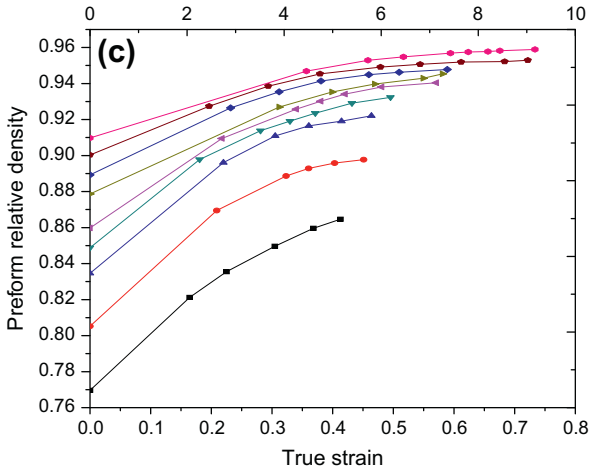

Fig. 3c. Variation of the relative density with respect to true strain for PM Al–4%Cu preforms.

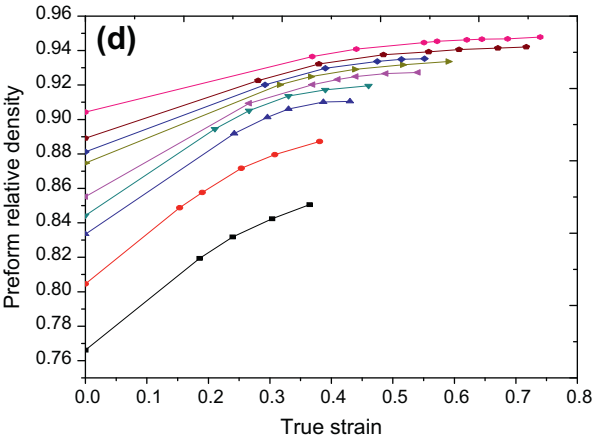

Fig. 3d. Variation of relative density with respect to true strain for PM Al–6%Cu composite.

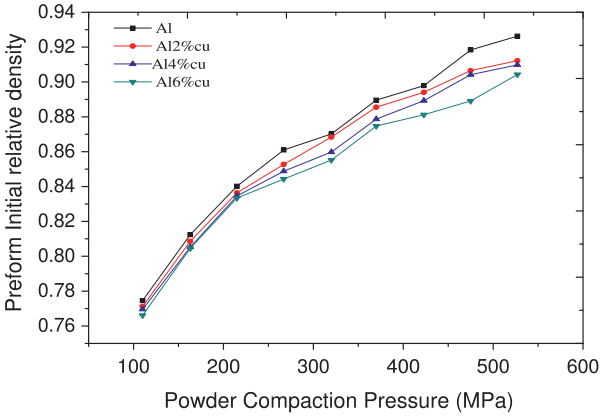

Fig. 4. Variation of the preform initial relative density with respect to powder compaction load for different content of copper in the composite.

results in large amount of densification. The effect of frictional constraint associated with less initial relative density preforms played a significant role for the increased densification rate.

Fig. 4 shows the variation of sintered densities with the addition of different weight percentage of copper content (0%, 2%, 4% and 6%) in the composite. The plot between the initial relative density

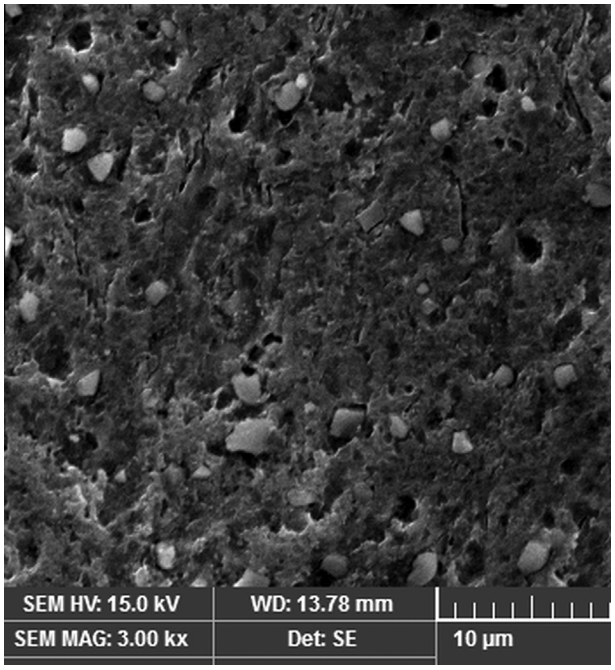

Fig. 5a. The SEM micrograph of sintered aluminium preforms of 87% initial relative density which shows spherically shaped pores before deformation.

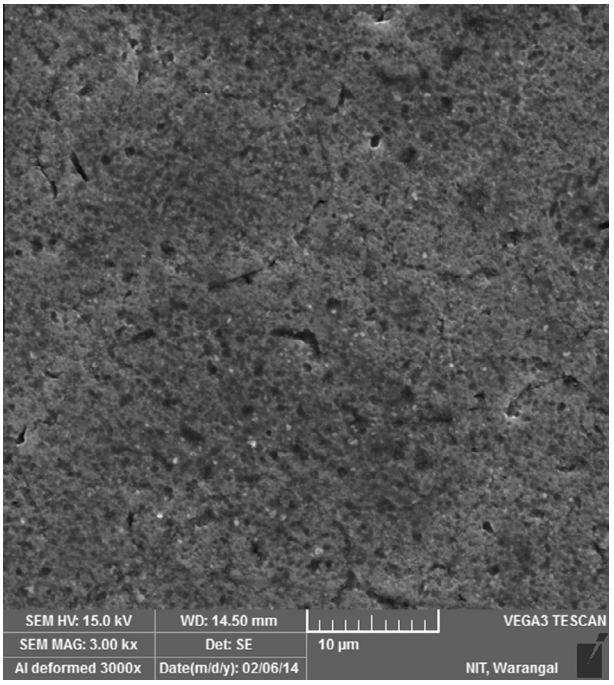

Fig. 5b. The SEM micrograph showing elongated and nearly cylindrical shaped pores of sintered aluminium preforms of 87% initial relative density and deformed to a true height strain of 0.5.

and the compaction load for different copper content in the composite shows a decrease in the sintered density with increase in the copper content, and the general observation of densification curves reveals an increase in the densification rate when the amount of copper content in the composite increases. The rate of densification varies at different stages of deformation. The amount of densification is higher at the initial stage of deformation and notably less at the final stage of deformation. This is due to less resistance of materials to deformation with the presence of more number of pores at the initial stage. At the final stage of deformation, the pores have got elongated perpendicular to the applied load axis and become cylindrical in shape that may act as a factor that increases the material resistance to the deformation. As the result, the amount of densification is less at the final stage of the deformation. Figs. 5a and 5b show the pore morphology of sintered aluminium preforms of 87% initial relative density before deformation and after deformed to a true height strain of 0.5 respectively. The shape of the pores left after sintering is nearly spherical in shape as sintered form, and after a true height strain of 0.5 deformations, the pore has become almost cylindrical in shape.

3.2. Forming limit diagram

The determination of different stress and strain components: axial, radial and hoop under triaxial state of stress were made using mathematical equations developed by Narayanasamy et al. [3,5,7]. From the logarithmic plot of true stress and true strain, the values of the apparent stain hardening exponent and strength coefficient were determined for various initial relative densities. The result reveals the apparent strain hardening exponent increase with decrease in the initial relative density and nears to the value of wrought materials as the initial relative density value approaches to higher values irrespective of the amount of copper content in the composite. Domination of the consolidation of pores over matrix hardening in the lesser relative density preforms is the reason for increase in the apparent strain hardening exponent. The presence of inherent porosity results in unhindered plastic flow of the material that increase work hardening of the preforms. Contrarily, the strength coefficient increases as the initial relative density increases. The results obtained are in similar pattern to the research findings of previous authors [9,14]. Furthermore, when the amount of copper content in the composite increases, both strain hardening exponent and strength coefficient values are increasing. This is due to the influence of increased number of inherent porosity left after sintering in the preforms.

A comparison was made on the results of n_a and K_a values of the PM preforms obtained in this research and the corresponding values in the earlier work [23] of cast aluminum–copper alloy of the similar composition. The strength coefficient value increases in similar pattern as the copper content increases in both PM and cast materials, but a different trend is observed on the values of strain hardening exponent. The strain hardening exponent value increases for both the cases up to copper content level of 4% in the aluminium matrix. Further increase in the copper content beyond 4% results in increased values of n_a in the PM preforms, but decreased in the cast material. The expected reasons are the presence of more inherent porosity in the PM preforms and grain refinement in the cast materials. The dominance in the effect of porosity and green size of the particulate on the work hardening behavior should be further investigated in the future work.

Figs. 6a–6d show plot of n_a and K_a with initial relative densities for 0%, 2%, 4% and 6% addition of copper in the composite. A decrease in n_a value and increase in K_a value with increase in initial relative densities were observed. The linear variation in n_a and K_a values were used to form the FLD for the extrusion of PM preforms. On all the cases, the plots of n_a and K_a values show a transition point on the slope of the linear line and called as CTD which demarcates the value of the minimum initial relative density of sintered preforms to get healthy extruded parts as revealed in the reference [9]. PM preforms with initial relative density higher than the CTD yield crack free extrudates. The CTD values occur 84% for Al, 85.3% for Al–2%Cu, 86% for Al–4%Cu and 87.5% for Al–6%Cu PM composites. These values determine the formability of the material to obtain healthy extrudates. Generally, the FLD is

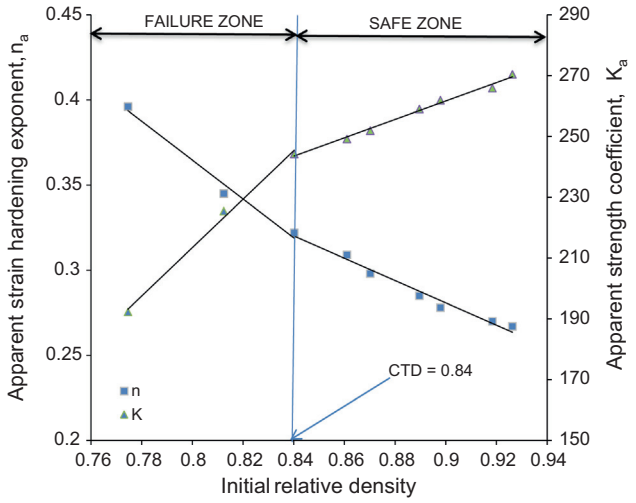

Fig. 6a. FLD for pure PM aluminium preforms obtained by plotting variation in the apparent strain hardening exponent and strength coefficient with respect to initial relative density.

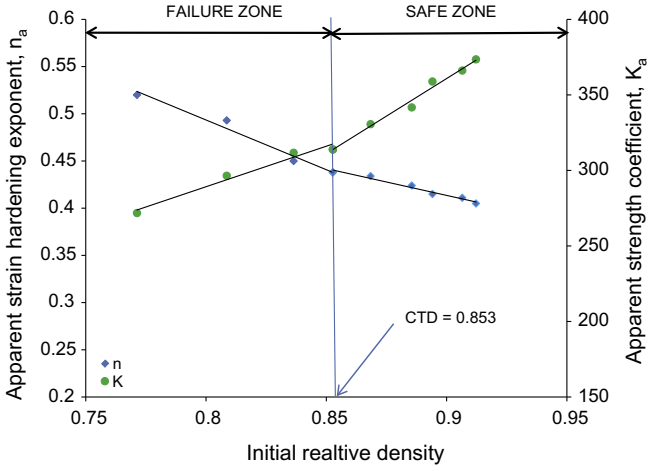

Fig. 6b. FLD for PM Al–2%Cu composite preforms obtained by plotting variation apparent stain hardening exponent and strength coefficient with respect to initial relative density.

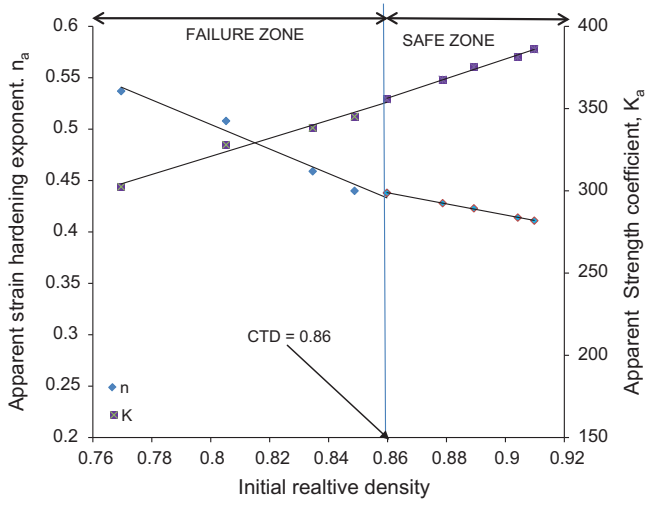

Fig. 6c. FLD of PM Al–4%Cu composite obtained by plotting variation in apparent strain hardening exponent and strength coefficient with respect to initial relative density.

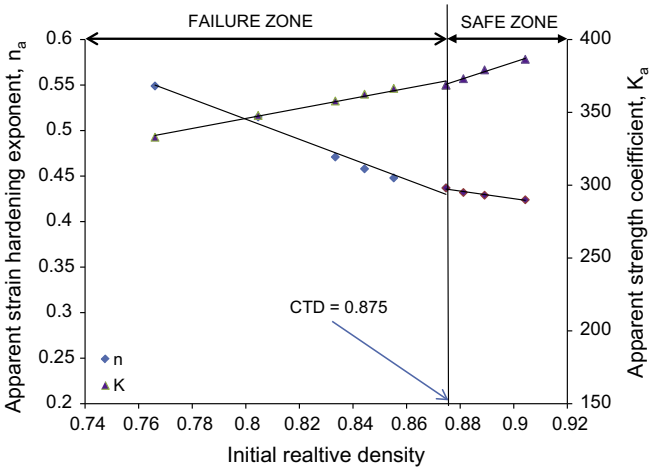

Fig. 6d. FLD for PM Al–6%Cu composite obtained by plotting variation in the apparent strain hardening exponent and strength coefficient with initial relative density.

divided into two safe zone and failure zone at the uniquely observable CTD value. The failure zone is characterized by the domination of consolidation of metal powders due to presence of more number of pores present in the composite, where as the safe zone is characterized by the domination of matrix work hardening over consolidation which leads to defect free cold extruded parts. More importantly, an increase in the value of CTD was observed when the copper content in the composite increases. As the result, the safe zone has become narrow and the failure zone has become wider. This is due to increase in the number of pores in the preforms with increase in the content copper particulates in the composite. Figs. 7a–d show the SEM photo of microstructure of sintered aluminum, Al–2%Cu, Al–4%Cu and Al–6%Cu composites.

3.3. Interface Friction factor (m)

During metal deformation, heat is generated due to friction at the interface between tool and work piece which has a significant impact on the formability of materials. The friction factor values between the tool and work piece interfaces were determined by generating friction calibration curve. The Male and Cockcroft [18] friction calibration curve was developed by using FEM software (DEFORM 2D). The reduction in the internal diameter (%) and reduction in height (%) values were plotted and made to fit the Male and Cockcroft calibration curve to determine the friction factor in dry condition. Fig. 8 shows the methodology that how the friction factor, m, was obtained using friction calibration curves for different initial relative density and content of copper in the composite.

As shown in Fig. 9, it is clearly evident that the interface friction factor between the tool and preform is dependent on the initial relative density and properties of the material. The result reveals that friction factor has increased as the value of initial relative density decreases due to presence of inherent porosity that leads to formation of dead-zone at the tool–metal interface. When the initial relative density increases and approaches to the value of the corresponding wrought material's, the material–tool interaction at the interface increases and results in a deceased friction factor. This is due to decrease in the n_a and increase in the K_a values which were obtained by the deformation test of cylindrical parts earlier in this work, and in consequence the dead metal zone at the tool-metal interface was decreased that resulted in low friction values. Venugopal et al. [24] was observed extremely high friction condi-

tions on PM iron preforms due to the influence of porosity, and reported decrease in n_a and increase in the K_a values as the relative density of preforms increase which yields lower friction values. In addition, the friction factor increases with increase in the content of copper in the composites.

Using the equations established elsewhere [19–21]; the friction factor is determined theoretically and compared with experimental results. Table 1 shows the comparison made between theoretical and experimental values of friction factor for different powder compaction load and content of copper in the composite.

From the results shown on the Table 1, it is clear that the value of friction factor, m, is decreasing with increase in the relative density and decrease in the copper content under both theoretical and experimental evaluations. This is due to the fact that preforms with more porosity undergo higher work hardening: matrix hardening and consolidation, in which the later has dominant effect and increases the lateral flow of materials during deformation, however the metal at the interface between tool and work piece undergoes limited plastic strain deformation (increased dead metal zone) because the pores act as a damper that hinders the flow of metal at the interface. As the result the interface friction increases.

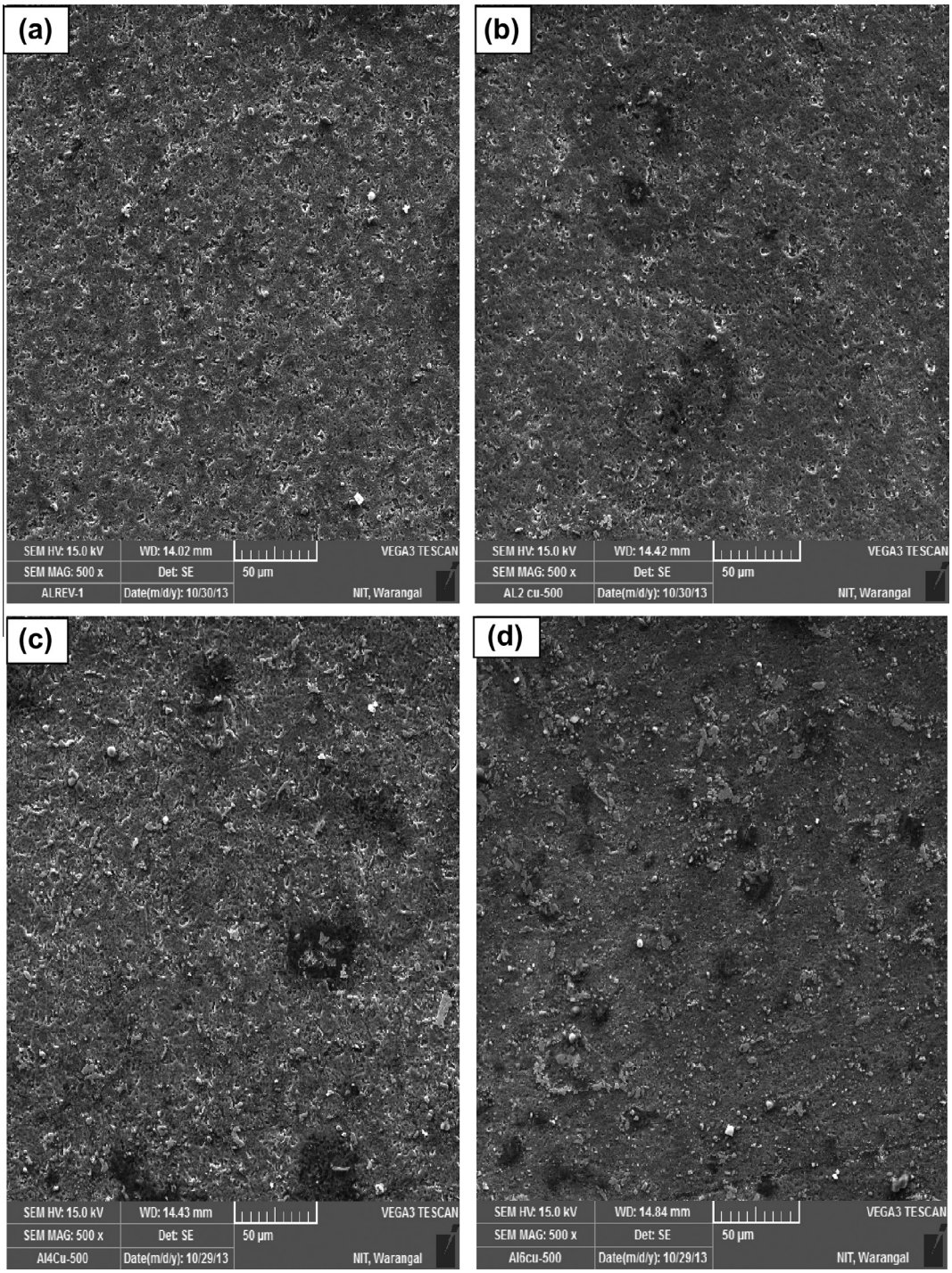

Fig. 7. SEM micrographs of the sintered (a) Al, (b) Al–2%Cu, (c) Al–4%Cu and (d) Al–6%Cu preforms.

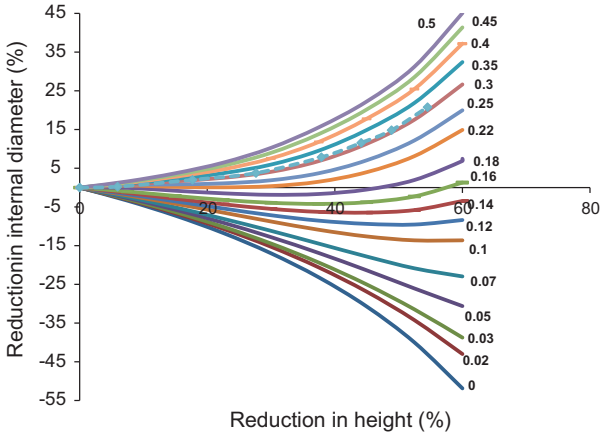

Fig. 8. Friction calibration curve for 0.93 initial relative PM aluminium preform obtained by plotting reduction in internal diameter (%) with respect to reduction in height (%).

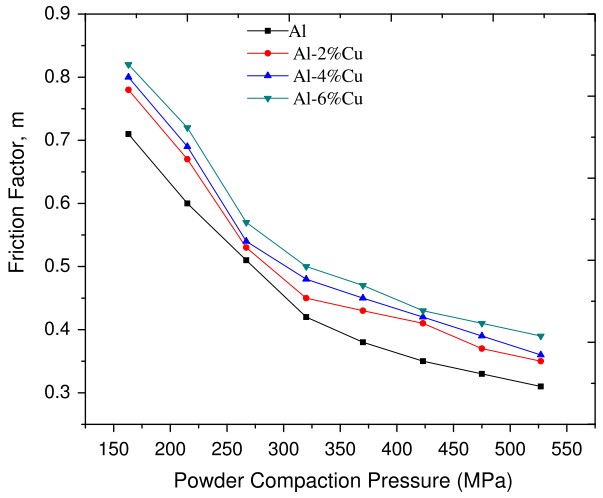

Fig. 9. Variation of friction factor (m) with respect to powder compaction pressure for PM pure Al, Al–2%Cu, Al–4%Cu and Al–6%Cu preforms.

4. Conclusions

The following conclusions can be drawn from the result and discussions.

(1) The initial relative density of the preforms decrease with increase in the content of copper in the composite for similar working conditions.

(2) The amount of densification increases with increase in the content of copper in the composite under similar working conditions.

(3) Non-uniform lateral constrained flow materials due to friction and the associated compressive hydrostatic stress are responsible for the densification.

(4) The friction factor between tool and work piece interface decreases with increase in the initial relative density for all the cases of copper content and increases with increase in the content of copper in the composite.

(5) With increase in the content of copper in the composite, the critical transition density values increases from 84% of pure aluminum to 85.3% with 2% copper addition, to 86% with 4% copper addition and 87.5% with 6% copper addition which narrow the safe working zone of the materials.

Acknowledgement

The authors would like to thank the technical staffs of National Institute of Technology, Warangal, India for helping to carry out the research work.

References

[1] Dieter GE. Mechanical Metallurgy. 3rd ed. New York: McGraw-Hill; 1981.
[2] Narayan S, Rajeshkannan A. Densification behaviour in forming of sintered iron-0.35% carbon powder metallurgy preform during cold upsetting. Mater Des 2011;32:1006–13.
[3] Narayanasamy R, Ramesh T, Pandey KS. Some aspects of workability studies in cold forging of pure aluminum powder metallurgy compacts. J Mater Sci Technol 2005;6(5):21:912.
[4] Bensam Raj J, Marimuthu P, Prabhakar M, Anandakrishnan V. Effects of sintering temperature and time intervals on workability behaviour of Al–SiC matrix P/M composite. J Adv Manuf Technol 2012;61:237–52.
[5] Narayanasamy R, Ramesh T, Pandey KS. Workability studies on cold upsetting of Al–Al_2O_3 composite material. Mater Des 2006;27:566–75.
[6] Zhang XQ, Peng YH, Li MQ, Wu SC, Ruan XY. Study of workability limits of porous materials under different upsetting conditions by compressible rigid plastic finite element method. J Mater Process Eng 2000;9:164–9.
[7] Narayansamy R, Ramesh T, Pandey KS. Some aspects of workability of aluminium–iron powder metallurgy composite during cold upsetting. J Mater Sci Eng 2005;391:418–26.
[8] Mohan Raj AP, Selvakumar N, Narayanasamy R, Kailasanathan C. Experimental investigation on workability and strain hardening behaviour of Fe–C–Mn sintered composites with different percentage of carbon and manganese content. Mater Des 2013;49:791–801.
[9] Chakravarthy P, Chakkingal Uday, Venugopal P. Influence of temperature on the forming limit diagrams of sintered PM preforms of steel. J Mater Sci Eng A 2008;482:395–402.
[10] Venugopal P, Annamalai S, Kannan KS, Srinivasan Sriram. Some aspects of cold extrusion of sintered copper preforms. J Mech Work Technol 1986;13:339–64.
[11] Seong-Guk Oh, Im Yong-Taek. An experimental study on densification of sintered iron P/M cylindrical billets in forward extrusion. J Mater Process Technol 1993;37:499–511.

Table 1
Experimental and theoretical friction factor (m) for various powder compaction pressures and content of copper in the composite.

Powder compaction load (MPa)	Friction factor (m)							
	Al preforms		Al2%Cu		Al4%Cu		Al6%Cu	
	Experimental	Theoretical	Experimental	Theoretical	Experimental	Theoretical	Experimental	Theoretical
527	0.31	0.36	0.35	0.38	0.36	0.41	0.39	0.42
475	0.33	0.38	0.37	0.39	0.39	0.42	0.41	0.43
423	0.35	0.39	0.41	0.4	0.42	0.43	0.43	0.44
370	0.38	0.41	0.43	0.42	0.45	0.44	0.47	0.46
320	0.42	0.43	0.45	0.44	0.48	0.46	0.5	0.49
267	0.52	0.5	0.53	0.51	0.54	0.53	0.57	0.55
215	0.6	0.58	0.67	0.62	0.69	0.65	0.72	0.69
163	0.71	0.66	0.78	0.73	0.8	0.76	0.82	0.78

[12] Venugopal P, Venkatraman S, Vasudevan R, Padmanabhan KA. Some failure studies in the hooker extrusion of sintered iron powder metallurgical preforms. J Mech Work Technol 1988;16:165–74.
[13] Narayanasamy R, Ramesh T, Pandey KS. An experimental investigation on strain hardening behavior of aluminium–3.5% alumina powder metallurgy composite preform under various stress states during cold upset forming. Mater Des 2007;28:1211–23.
[14] Venugopal I P, Venkatraman S. Some aspects of n_a and K_a in the prediction of cold extrusion forces of sintered powder metallurgical preforms. J Mech Work Technol 1988;17:113–7.
[15] Das S, Behera R, Datta A, Majumdar G, Oraon B, Sutradhar G. Experimental investigation on the effect of reinforcement particles on the forgeability and the mechanical properties of aluminum metal matrix composites. J Mater Sci Appl 2010;1:310–6.
[16] Madhusudan S, Sarcar MMM, Bhargava NRMR, Sunil Ratna Kumar K. Fabrication and deformation studies of Al–Cu composite metallic materials. Indian J Eng Mater Sci 2012;10:175–8.
[17] Mondolfo LF. Aluminum Alloys: Structures and Properties. London: Butterworths & Co Publishers Ltd; 1976.
[18] Male AT, Cockcroft MG. A method for the determination of coefficient of friction of metals under bulk plastic deformation. J Ins Met 1964/1965;93:38–46.
[19] Ettouney OM, Stelson KA. An approximate model to calculate foldover and strains during cold upsetting of cylinders Part II: Use of the foldover model to estimate friction. J Eng Ind 1990;112:267–71.
[20] Male AT, Depierre V. The validity of mathematical solutions for determining friction from the ring compression test. J Lubrication Technol 1970;92(3): 389–95.
[21] Avitzur B. Metal forming: processes and analysis. New York: McGraw Hill Inc.; 1968. p. 81–102.
[22] Kandavel TK, Chandramouli R, Shanmugasundaram D. Experimental study of the plastic deformation and densification behaviour of some sintered low alloy P/M steels. Mater Des 2009;30:1768–76.
[23] Babu Rao J, Kamaluddin Syed, Appa Rao J, Sarcar MMM, Bhargava NRMR. Finite element analysis of deformation of aluminum–copper alloys. Mater Des 2009;30:1298–309.
[24] Venugopal P, Venkatraman S, Vasudevan R, Padmanabhan KA. Ring-compression tests on sintered iron preforms. J Mech Work Technol 1988;16:51–64.